Compatibility of Alumina with eutectic Pb-Li alloy

Uttam Jain*, Abhishek Mukherjee, and R. Tewari

[1]Materials Group, Bhabha Atomic Research Centre, Mumbai-400085, India

Abstract

The use of eutectic lead lithium ($Pb_{83}Li_{17}$) alloy as a coolant-cum-tritium breeder in fusion reactors presents challenges related to magneto-hydrodynamic drag (MHD) and corrosion. To address these issues, alumina (Al_2O_3) is proposed as a ceramic coating material. This study focuses on the characterization of $Pb_{83}Li_{17}$ alloy and its interaction with Al_2O_3 at the reactor's operating temperature. The investigation employs EPMA, XRD, and thermal analysis techniques. Results indicate that alumina can interact with $Pb_{83}Li_{17}$ alloy at 550 ºC, even in a high-purity argon atmosphere. The role of oxygen in this interaction process is also discussed. These findings contribute to the understanding of materials for fusion power applications.

Key words: Lead-lithium eutectic, Alumina, Compatibility, Diffusion, Thermal analysis.

1. Introduction

Liquid lead lithium alloy ($Pb_{83}Li_{17}$) has emerged as a promising candidate for coolant, tritium breeder, and neutron multiplier applications in the blanket systems of advanced fusion reactors, including the International Thermonuclear Experimental Reactor (ITER) and Fusion Power Reactors (FPR) [1-5]. However, a critical challenge in the development of liquid metal-cooled blanket systems lies in ensuring compatibility between the liquid metal and structural materials.

Currently, reduced activation ferritic martensitic (RAFM) steels are employed as structural materials in fusion reactor test blanket systems [6-8]. Among the key issues facing Pb-Li cooled blankets in ITER are tritium permeation, corrosion, and magneto-hydrodynamic drag (MHD) effects, which are actively being addressed [1,5,8-11]. To minimize the effect of tritium permeation, permeation barriers are installed and to tackle the MHD effect and corrosion, blanket / structural materials are being coated with ceramics. These ceramic coatings serve a dual purpose by preventing direct contact between the materials and the liquid metal and electrically decoupling them from the conductive liquid metal flow within the magnetic field [1, 2, 3, 5, 8, 9-14].

The exploration of various ceramic coatings for $Pb_{83}Li_{17}$ systems includes oxides (Al2O3, Cr_2O_3, Y_2O_3, SiO_2, CaO, and MgO), nitrides (AlN, TiN), and carbides (β-SiC, TiC) [2, 9, 10]. Among these options, aluminum oxide (Al_2O_3) stands out as a prime candidate due to its exceptional thermochemical stability, high electrical resistivity, radiation resistance, and excellent compatibility with $Pb_{83}Li_{17}$ alloy [8, 11, 15-18].

In ITER and FPR, the coolant $Pb_{83}Li_{17}$ alloy operates within the temperature range of 450-550 °C. Ensuring compatibility between alumina and the liquid $Pb_{83}Li_{17}$ alloy at this temperature range is a critical consideration. Hubberstey et al. [2] reported the formation of Li_2O(s) in $Pb_{83}Li_{17}$ alloy in the presence of oxygen, despite the low activity of Li. Their thermodynamic calculations suggested that oxides like alumina should be thermodynamically stable in oxygen-saturated Pb83Li17. Subsequently, Pint et al. [15, 19, 20] found that the interaction of $Pb_{83}Li_{17}$ with alumina in an argon atmosphere at 800 °C for 1000 hours resulted in the formation of $LiAlO_2$(s) compound. Notably, the reaction kinetics were slow, likely due to the limited supply of oxygen (from impurities in argon or dissolved oxygen in $Pb_{83}Li_{17}$).

The interaction of Al_2O_3 with liquid $Pb_{83}Li_{17}$ alloy at the fusion reactor's operating temperature range (450-550 °C) remains relatively understudied in open literature. This investigation focuses on the heating/cooling behavior of $Pb_{83}Li_{17}$ alloy and its interactions with alumina within this temperature range. The role of oxygen in the interaction process is also examined. Experiments were conducted in both the presence and absence of oxygen atmosphere, achieved through high purity argon atmosphere from a cylinder and/or high vacuum (10^{-6} mbar) to ensure an oxygen-free environment, while experiments in air provided a continuous supply of oxygen. The study utilizes EPMA, XRD, and thermal analysis techniques to examine the interaction between liquid $Pb_{83}Li_{17}$ alloy and alumina.

2. Experimental

2.1 Materials

Homogeneous $Pb_{83}Li_{17}$ alloy was prepared in-house at the Materials Group, BARC, using a patented technology. The alloy was contained in a tantalum crucible and sealed in an evacuated quartz ampoule, then annealed at 200 °C for 48 hours prior to use. Powder X-ray diffraction (XRD) analysis was performed using an Inel instrument with Cr-Kα radiation to characterize the alloy. The obtained d-spacings were compared with those listed in the PCPDF database for

phase identification. Compositional analysis was conducted using a CAMECA SX 100 Electron Probe Micro Analyzer (EPMA). The lithium content in the lead lithium alloy was determined using the inductively coupled plasma atomic emission spectroscopy (ICP-AES) technique. The samples were dissolved in 2% HNO_3 and analyzed using ICP-AES for lithium content measurement.

2.2 Interaction studies of alumina with $Pb_{83}Li_{17}$ alloys

2.2.1 Heating $Pb_{83}Li_{17}$ alloys in an alumina boat

The initial interaction studies involved melting 50 g of lead lithium alloy in an alumina boat at 550 °C for 6 hours under a flowing high-purity argon atmosphere. After solidification, the resulting melt was found to adhere to the surface of the alumina boat. The interface between alumina and the solidified $Pb_{83}Li_{17}$ was carefully sliced using a diamond saw and subsequently subjected to compositional analysis using the Electron Probe Micro Analyzer (EPMA).

2.2.2 Thermal equilibration of $Pb_{83}Li_{17}$ alloys with alumina powders in sealed quartz ampoule

To further investigate the interaction, dried alumina powders were mixed with small chunks of $Pb_{83}Li_{17}$ alloy at a weight ratio of 1:5. Two sets of samples were prepared:

(1) The mixture was wrapped in tantalum foil, and the foil was sealed in a quartz ampoule that was then evacuated to a pressure of 4×10^{-6} mbar.

(2) The mixture was placed on an alumina boat.

Both sets of samples were heated in a furnace at 550 ºC for 48 hours to achieve thermal equilibration. This study aimed to examine the effect of oxygen ingress on the interaction behavior between alumina and $Pb_{83}Li_{17}$ alloy.

2.2.3 Thermal analysis studies

Simultaneous thermal curves (TG-DTA) were obtained using a Setaram thermoanalyzer. Small chunks of $Pb_{83}Li_{17}$ alloy, each weighing 170 mg, were subjected to heating from 50 to 500°C at a heating rate of 5 °C/min. This thermal analysis was conducted in an alumina cup under two different conditions:

(1) Flowing High Purity Argon Atmosphere: The sample was heated in an environment of high purity argon gas, and argon was continuously flushed over the sample for 12 hours prior to heating.

(2) Air Atmosphere: The sample was heated in ambient air without any additional protective gas environment.

TG-DTA curves were recorded for both scenarios to study the thermal behavior of $Pb_{83}Li_{17}$ alloy under flowing argon and air atmospheres.

3. Results and discussions

3.1 Characterization of the starting $Pb_{83}Li_{17}$ alloy

The X-ray diffraction (XRD) pattern of the solid $Pb_{83}Li_{17}$ alloy exhibited similarities to that of pure lead (PCPDF no: 04-0686), with a slight shift in peak positions towards higher 2θ values. The alloy was found to crystallize in a cubic crystal structure, with a lattice parameter of a = 4.9342 Å, compared to the reported value of 4.950 Å for pure Pb [5]. The decrease in d-spacing is attributed to the formation of a lead lithium solid solution, where smaller lithium atoms (atomic size: 156 pm) substitute larger lead atoms (atomic size: 175 pm) in the lattice, causing it to contract [21]. Despite annealing the sample at 200 °C for 120 hours in an evacuated quartz ampoule, no XRD peaks corresponding to the co-existing second phase PbLi(s) were observed.

PbLi is known to be a rhombohedral phase with a slightly distorted CsCl structure [22]. Previous X-ray patterns from room temperature showed a complex rhombohedral phase that transformed into a simple cubic phase as PbLi was heated [22]. It is plausible that the PbLi phase retains its cubic structure at room temperature, explaining its absence in the XRD pattern.

The scanning electron microscopy (SEM) backscattered electron image of the $Pb_{83}Li_{17}$ alloy (Fig1) revealed two distinct phases. The brighter phase corresponded to the Pb(Li) solid solution containing approximately 1 at % Li, while the darker phase corresponded to the PbLi(s) phase. The composition of Li in these two phases could not be precisely ascertained due to its low atomic number (Z). Nevertheless, ICP-AES chemical analysis indicated that the $Pb_{83}Li_{17}$ alloy contained 16.2 ± 0.2 atom % of Li.

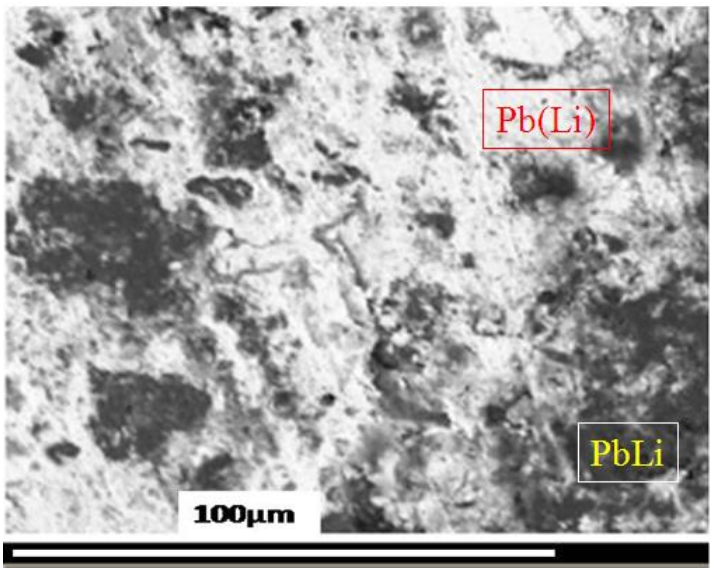

Fig. 1 SEM image of $Pb_{83}Li_{17}$ alloy showing two phases corresponding to PbLi and Pb(Li)

3.2 Diffusion studies of $Pb_{83}Li_{17}$ alloy in alumina boat

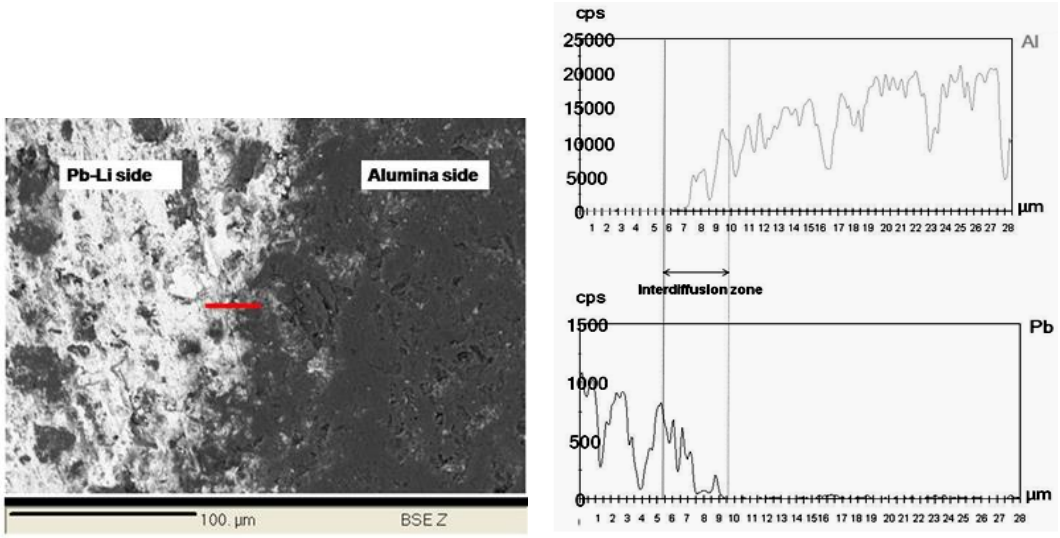

Fig.2 (a) Back scattered electron (BSE) EPMA image of Pb-Li alloy and alumina interface

(b) EPMA line scans of Pb-Li alloy and alumina interface depicting Al and Pb counts

The diffusion characteristics of the $Pb_{83}Li_{17}$-Al_2O_3 interface were studied by melting the alloy in an alumina boat, and the investigation was carried out using an electron probe micro-analyzer (EPMA). Figure 2a displays the backscattered electron (BSE) EPMA image of the interface. The white phase observed on the lead-lithium side corresponds to the Pb(Li) phase, while small grayish islands represent the PbLi phase. The darker phase on the right side of the

interface corresponds to alumina. Notably, due to limitations in EPMA, the presence of lithium could not be detected, and thus, compositional analysis focused solely on lead and aluminum. Figure 2b presents the EPMA line scan of the interface, illustrating the counts of Pb and Al. A clear inter-diffusion zone, approximately 4μm in width, where counts corresponding to both lead and aluminum were present, is evident. The presence of inter-diffusion indicates the potential interaction between $Pb_{83}Li_{17}$ and Al_2O_3 at the interface.

3.3 Thermal equilibration studies of $Pb_{83}Li_{17}$ alloy with alumina powders

During the heating schedule, the $Pb_{83}Li_{17}$ alloy melted, reacted with the alumina and was allowed to solidify. Interestingly, the reacted alumina powder was not embedded inside the melt; rather, they could be easily separated. As a result, sample analysis for XRD was conducted separately for the solidified alloy (Fig. 3a and b) and the reacted alumina powder (Fig. 4a and b). The XRD analysis of the solidified $Pb_{83}Li_{17}$ alloy heated with alumina in vacuum (Fig. 3a) showed that all the peaks still corresponded to the starting alloy, indicating no significant changes in the alloy's crystalline structure. However, when the solidified metal was heated in air (Fig. 3b), the XRD pattern corresponded to that of pure lead along with the appearance of PbO peaks (PCPDF: 720094). This indicates that Li in the Pb83Li17 alloy has completely oxidized, leaving behind pure Pb, which has also partly oxidized to give rise to the peaks of PbO. The oxidation of lithium and partial oxidation of lead in the presence of air suggests the occurrence of a chemical reaction between the alloy and the surrounding atmosphere during the heating process.

The XRD patterns of the reacted alumina powder in vacuum and in air are presented in Figure 4a and Figure 4b, respectively. The XRD pattern of the sample equilibrated in vacuum (Figure 4a) corresponded exactly to pure alumina (PCPDF: 461212), indicating that alumina does not react with the $Pb_{83}Li_{17}$ alloy under vacuum conditions. However, when alumina was heated in air (Fig. 4b), additional peaks of $LiAlO_2$ (PCPDF: 731338) were observed alongside the alumina peaks. Notably, no separate phase of Li_2O was detected in the XRD pattern (Figure 4b), leading to the conclusion that at 550 °C, Al_2O_3 interacts with $Pb_{83}Li_{17}$ alloy (under the ingress of oxygen) following the reaction:

$Li_2O(s) + Al_2O_3(s) \rightarrow 2LiAlO_2(s)$ ($\Delta G°$ 550 °C = -117 kJ) …………………….. (1)

Previous studies by Pint et al. [15] reported the temperature for Pb83Li17 alloy interaction with alumina to form $LiAlO_2$(s) compound under an argon atmosphere to be 800 °C. However, our

findings reveal that the interaction between Pb83Li17 alloy and alumina to form LiAlO2 can occur at a lower temperature of 550 °C, provided there is a sufficient supply of oxygen. Notably, in vacuum conditions (4×10^{-6} mbar), no visible reaction between $Pb_{83}Li_{17}$ and alumina was observed even after 48 hours. An inert gas like argon or helium may contain trace amounts of oxygen, and when used as flowing gas in a reactor for prolonged durations, it would ensure a constant supply of oxygen. This gradual oxygen supply would eventually lead to the formation of $LiAlO_2$ even at 550 °C, although at a slower rate compared to that observed in air. To investigate the interaction behavior in an inert gas, thermal studies as described in the following section (Section 3.4) were undertaken.

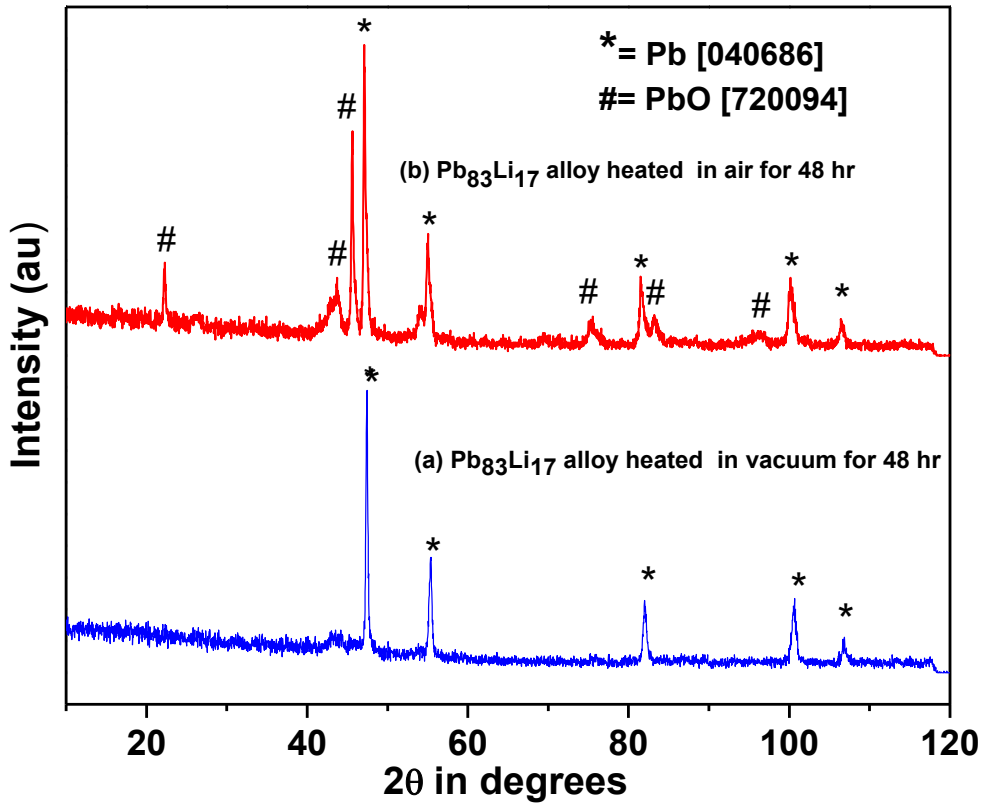

Fig.3XRD patterns of lead lithium alloy thermally equilibrated with alumina powder at 550 °C for 48h (a) in vacuum (b) in air

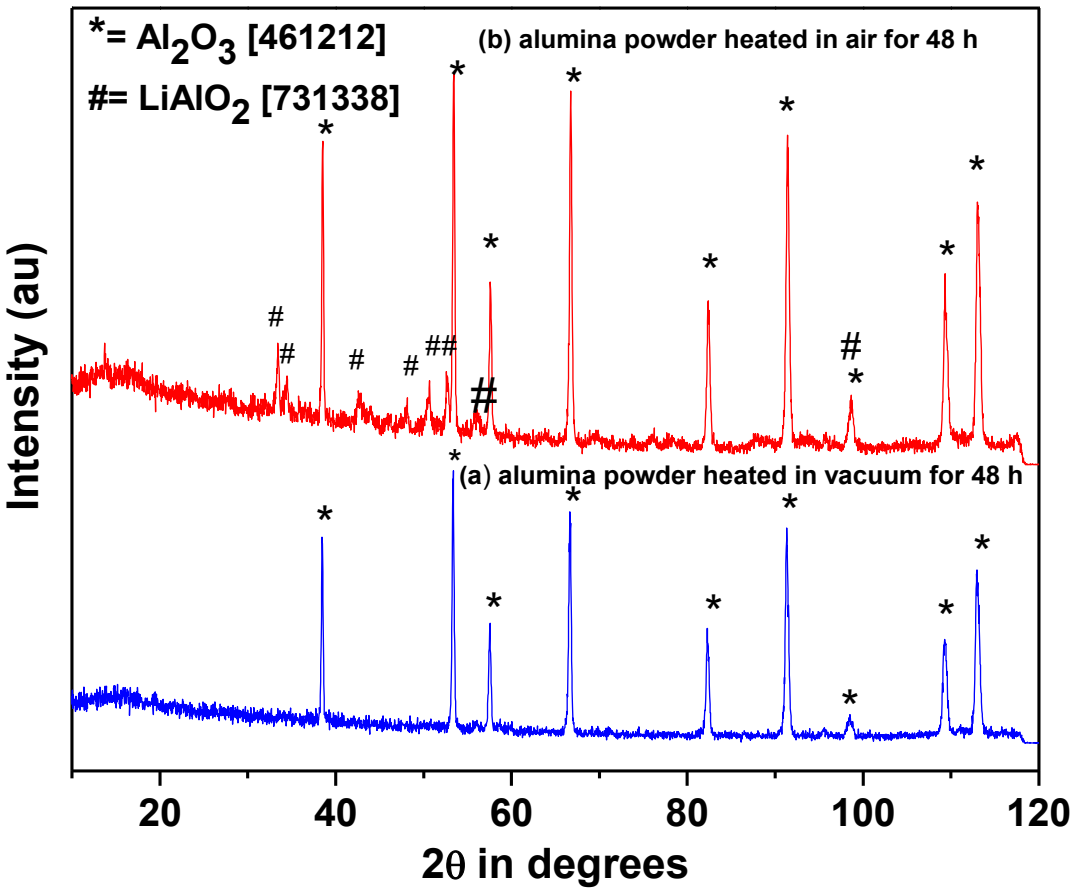

Fig.4 XRD patterns of alumina thermally equilibrated with lead lithium alloy at 550 °C for 48h (a) in vacuum (b) in air

3.4 Thermal analysis (TG-DTA) studies

Fig. 5a displays the TG-DTA plot obtained from the $Pb_{83}Li_{17}$ alloy heated in an alumina cup under a flowing argon atmosphere. Two endothermic peaks were observed with onset temperatures at 219 °C and 229 °C. The weak peak at 219 °C is attributed to the phase transition in the PbLi(s) phase, while the strong peak at 229 °C corresponds to the eutectic melting of the alloy. The absence of any major endothermic peak following the eutectic peak suggests that the starting Pb83Li17 alloy was close to its eutectic composition.

The simultaneous TG-plot (weight change) showed a mass gain of about 1.25 mg in the temperature range of 230 to 500 °C, beyond the eutectic melting temperature. This mass gain is attributed to the preferential oxidation of Li metal in the molten alloy. The observed weight gain (1.26 mg) agrees well with the expected mass gain if all the Li in the 170 mg $Pb_{83}Li_{17}$

alloy was considered to be oxidized. Notably, the weight gain indicates that liquid lead was not getting oxidized in the argon atmosphere.

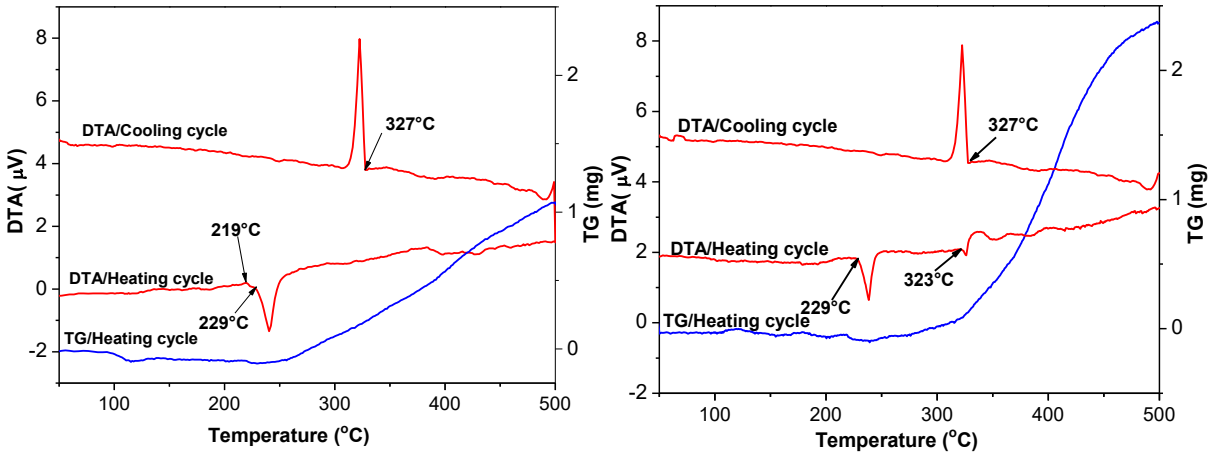

Fig.5 (a) Simultaneous TG-DTA plot of $Pb_{83}Li_{17}$ alloy heated upto 500 °C in argon
(b) TG-DTA plot of $Pb_{83}Li_{17}$ alloy heated upto 500°C in air

The observed oxidation of Li in the flowing argon atmosphere can be explained by the equilibrium oxygen potential of the Li/Li_2O system. The calculated oxygen potential for the Li/Li_2O system [23] is found to be of the order of 10^{-61} atm at 220 °C, suggesting that the oxygen potential achieved by the flow of argon in the system is significantly higher than the required oxygen potential for the oxidation of Li.

Furthermore, it was observed that the rate of mass gain due to the preferential oxidation of Li in the $Pb_{83}Li_{17}$ alloy increased above 370 °C, accompanied by the appearance of a small endothermic peak. This peak is attributed to the rapid oxidation of Li, leading to the generation of pure Pb metal, which subsequently undergoes in-situ melting, resulting in the observed endothermic peak. The cooling curve recorded for the system shows a single exothermic peak at 327 °C, which is likely due to the freezing of liquid Pb. Importantly, no other exothermic peak besides the eutectic freezing was observed, indicating that all the Li metal had oxidized during the heating cycle, leaving only Pb metal in the sample.

Fig. 5b displays the TG-DTA plot recorded in static air. The DTA plot in Fig. 5b exhibited an endothermic peak resulting from a superimposed phase transition and the eutectic melting effect, along with an additional small endothermic peak at 323 °C (in contrast to 370 °C observed in Fig 5a). The appearance of this DTA peak in air can be attributed to the melting of

lead metal formed due to the preferential oxidation of the Li component at a lower temperature compared to the argon-heated sample.

In the TG plot, the mass gain curve shows a total mass gain of 2.5 mg for the 170 mg sample in the temperature range of 230 to 500 °C when heated in air. This total mass gain can be divided into two components: a mass gain of 1.26 mg, attributed to the complete oxidation of Li (17 at %), forming Li_2O(s), and the remaining 1.24 mg due to the partial oxidation of lead, forming PbO(s).

The DTA plot in the cooling cycle showed one exothermic peak corresponding to the crystallization of liquid Pb, similar to the DTA plot recorded in a flowing argon atmosphere. However, the relative peak intensity due to the freezing of Pb(l) decreased compared to the argon-heated sample, suggesting a smaller amount of metallic Pb was present in this alloy after heating in air. These results support the occurrence of preferential oxidation of Li in the presence of oxygen, leading to the formation of Li_2O(s) and PbO(s) phases, along with a reduction in metallic Pb content.

It is important to note that no exothermic peaks corresponding to the formation of LiAlO2 were observed in the thermal studies of $Pb_{83}Li_{17}$ alloy heated in either argon or air. This lack of observable exothermic peaks could suggest either a low exothermicity of the reaction or an extremely slow reaction rate. However, the thermal studies did indicate the formation of Li_2O at 550 °C, even in flowing high purity argon gas. This suggests that with time, Li_2O is likely to react with alumina to form $LiAlO_2$, as discussed in Section 3.3.

In the context of ITER, where experiments are expected to last only for 1000 seconds, the reaction between alumina and $Pb_{83}Li_{17}$ alloy may not be detrimental. However, in future fusion power reactors, where alumina and $Pb_{83}Li_{17}$ alloy are expected to be in contact for longer durations under the flow of high purity inert gas, alumina coating may not be an entirely suitable choice. Further research is required to explore new and more compatible coating materials for such applications.

4. Conclusions

The manuscript investigates the interaction between liquid $Pb_{83}Li_{17}$ alloy and Al_2O_3 at fusion reactor operating temperatures (400-550 °C). The role of oxygen in this interaction was also examined. The main findings are as follows:

- Under vacuum conditions (4×10^{-6} mbar) at 550 °C for 48 hours, there was no interaction observed between liquid $Pb_{83}Li_{17}$ alloy and Al_2O_3.

- When heated in air at 550 °C for 48 hours, both lead and lithium in the liquid Pb83Li17 alloy were oxidized. Additionally, in the presence of flowing argon, rapid oxidation of lithium occurred beyond the eutectic melting temperature (235 °C).

- Alumina was found to react with Li_2O at 550 °C, resulting in the formation of the $LiAlO_2$ compound. The reaction occurred more rapidly in the presence of oxygen and at a slower rate in the presence of flowing argon.

These observations provide valuable insights into the behavior of $Pb_{83}Li_{17}$ alloy in contact with alumina under different conditions, shedding light on the importance of oxygen and inert gas environments in the interaction process.

Acknowledgment

The authors would like to acknowledge the support of the Indian TBM program for structural materials, which made this investigation possible. Special thanks are extended to Dr. Pranesh Sengupta from MSD, BARC, for his valuable assistance in the EPMA analysis, and Dr. Ratiknat Mishra for conducting the TG-DTA experiments. Their contributions greatly enriched the quality and outcomes of this study.

References

1. B.A. Pint, Mater. Sci. Forum. 595-598 (2008) 549-558.
2. P. Hubberstey, J. Nucl. Mater. 247 (1997) 208-214.
3. S. Malang, R. Mattas, Fusion Eng. Des. 27 (1995) 399-406.
4. S. Malang, H. Deckers, U. Fischer, H. John, R. Meyder, P. Norajitra, J. Reimann, H. Reiser, K. Rust, FusionEng. Des. 14 (1991) 373-399.
5. S. Malang, H.U. Borgstedt, E.H. Farnum, K. Natesan, I.V. Vitkovski, Fusion Eng. Des. 27 (1995) 570-586.
6. Y. Wu, the FDS Team, Fusion Eng. Des. 82 (2007) 1893-1903.
7. Y. Wu, the FDS Team, J.Nucl. Mater. 367–370 (2007) 1410-1415.
8. Z. Guoa, Q. Huang, Z. Yan, Fusion Eng. Des. 85 (2010) 1469-1473.

9. P. Hubberstey, T. Sample, J. Nucl. Mater. 248 (1997) 140-146.
10. P. Hubberstey, T. Sample, A. Terlain, Fusion Techn. 28 (1995) 1194.
11. Y. Ueki, T. Kunugi, N.B. Morley, M. A. Abdou, Fusion Eng. Des. 85 (2010) 1824-1828.
12. D.L. Smith, J. Konys, T. Muroga, V. Evitkhin, J.Nucl. Mater. 307–311 (2002) 1314-1322.
13. Y.Y. Liu, D.L. Smith, J.Nucl. Mater. 141-143 (1986) 38-43.
14. I.R. Kirillov, I.V. Danilov, S.I. Sidorenkov, Yu.S. Strebkov, R.F. Mattas, Y. Gohar, T.Q. Hua, D.L. Smith, Fusion Eng.Des. 39–40 (1998) 669-674.
15. B.A. Pint, K.L. More, J. Nucl. Mater. 376 (2008) 108-113.
16. T. Wang, J.Pu, C. Bo, L.Jian, Fusion Eng. Des. 85 (2010) 1068-1072.
17. G.W. Hollenberg, E.P. Simonen, G. Kalinin, A. Terlain, Fusion Eng. Des. 28 (1995) 190-208.
18. D. Levchuk, F. Koch, H. Maier, H. Bolt, J. Nucl. Mater. 328 (2004) 103-106.
19. B.A. Pint, J. Nucl. Mater. 417 (2011) 1195-1199.
20. B.A. Pint, K.A. Unocic, J.Nucl. Mater. 442 (2013) 572-575
21. N. W. Alcock, Bonding and structure -structural principles in inorganic and organic chemistry, Ellis Horwood, Series in Inorganic Chemistry, Ellis Horwood, Chichester, 1990.
22. A. Zaklin, W.J. Ramsey, J.Phys. Chem. 61(1957) 1413-1415
23. G.V. Belov, B.G. Trusov, ASTD “Computer aided reference book in thermodynamical, thermochemical and thermophysical properties of species, Version 2.0, Moscow, (C) 1983-1995.
24. http://www.iter.org/newsline/122/182
25. J. Jordanova, U. Fischer, P. Pereslavtsev, Fusion Eng. Des. 84 (2009) 985–988
26. A. K. Suri, N. Krishnamurthy, I. S. Batra, J. Physics, Conference Series 208 (2010) 012001